

# Design of a low-cost, interactive, holographic optical tweezers system

E. Pleguezuelos, J. Andilla, A. Carnicer, E. Martín-Badosa,  
S. Vallmitjana and M. Montes-Usategui

Universitat de Barcelona, Departament de Física Aplicada i Òptica,  
Martí i Franquès 1, 08028 Barcelona, Spain

## ABSTRACT

The paper describes the design of an inexpensive holographic optical tweezers setup. The setup is accompanied by software that allows real-time manipulation of the sample and takes into account the experimental features of the setup, such as aberration correction and LCD modulation. The LCD, a HoloEye LCR-2500, is the physical support of the holograms, which are calculated using the fast random binary mask algorithm. The real-time software achieves 12 fps at full LCD resolution (including aberration correction and modulation) when run on a Pentium IV HT, 3.2 GHz computer.

**Keywords:** Optical Trapping, Digital holography

## 1. INTRODUCTION

This paper describes the design procedure for a real-time, reconfigurable, holographic optical tweezers setup. The device has been built using low-cost components, for a total amount not in excess of 10,000 € (about \$12,500). The experimental set-up is based on a Motic AE31 inverted microscope using a 100x N.A. 1.25 objective, illuminated by a 532 nm 120 mW Viasho laser. The sample plane can be observed with a CCD camera through the dichroic mirror.

A HoloEye LC-R 2500 reflective SLM is been used to display the holograms that generate the desired trap pattern at the focal plane of the objective lens. The modulator is placed at 45° with respect to the incident beam, which allows better control of the different SLM operating modes. The device has been fully characterized in order to obtain an almost phase-only configuration that optimizes light efficiency. For a wavelength of 532 nm, we have found a phase modulation of  $2\pi$ , where the amplitude is almost constant. We have observed that the traps show astigmatic behavior when focused at different planes. This may be caused by the SLM panel not being completely flat and having a small optical power. This problem can be overcome by adding the proper phase pattern to all the holograms.

The traps are controlled by means of a fast algorithm that directly gives the desired hologram with straightforward computations. The algorithm can also be used to modify any existing hologram very quickly and it does not produce ghost traps or replicas. The control software is implemented in Java and is capable of displaying 1024×768 pixel holograms at an average rate of 12 Hz (including aberration correction of the SLM and compensation of the operating curve nonlinearities) when run on a Pentium IV HT, 3.2 GHz computer.

## 2. THE OPTICAL SETUP

In this section we describe the design of the experimental setup. The setup is shown in Figure 1(a). It is based on a Motic AE31 inverted microscope using a 100x N.A. 1.25 objective. This microscope has been modified to introduce the laser beam through the epifluorescence port. The laser is a continuous-wave, frequency-doubled Nd:YVO<sub>4</sub> laser of 120 mW from Viasho Technology ( $\lambda = 512$  nm).

A pinhole filters high frequency terms in the Fourier plane of the expander lens (8mm of focal length) and the beam is collimated with a 75 mm focal lens. Taking into account that the beam waist is 0.9 mm wide and the

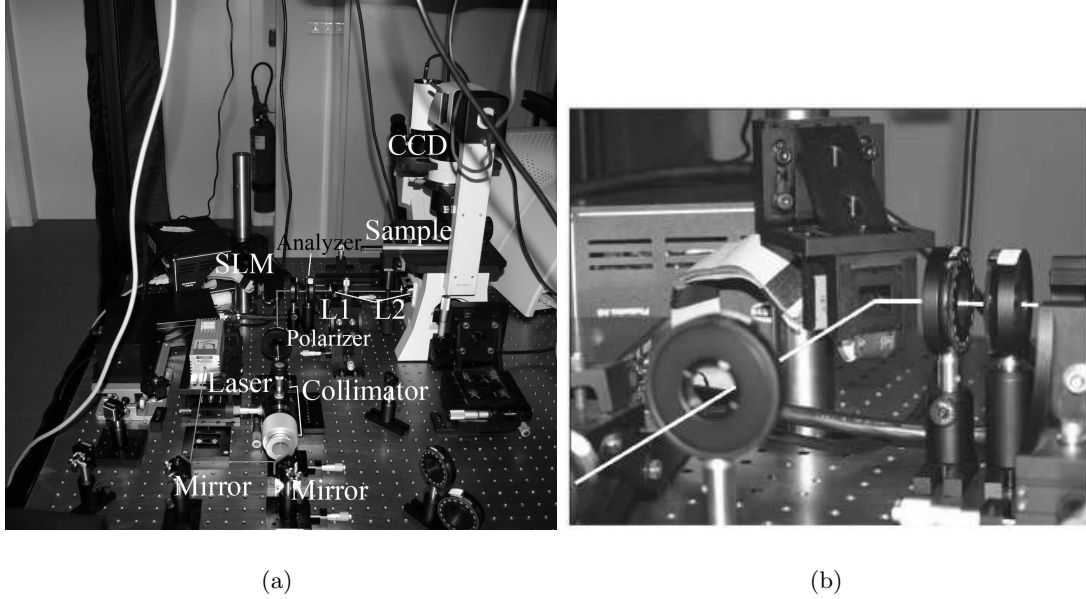


**Figure 1.** (a) Experimental setup for the generation of holographic optical tweezers. L1 and L2 are the two lenses of the telescope, while the collimator is a system comprising an expander lens, a pinhole and a second lens which collimates the beam. (b) The modulator placed in the setup with an inclination angle of  $45^\circ$  with respect to the beam direction.

magnification of the collimator system is  $8/75$  (the focal ratio of the collimator), the beam is thus expanded to 8.7 mm.

The reflective modulator, a HoloEye LC-2500, is placed at  $45^\circ$  with respect to the beam direction (as seen in Figure 1(b)). This inclination avoids the need for a beam-splitter, which would reduce the efficiency to 25%. The experimental characterization of the modulation curve has been obtained with this inclination angle. As the illuminated area is  $8.7 \times (8.7 \times \sqrt{2})$  mm and the HoloEye area is  $14.6 \times 19.6$  mm, the borders of the modulator are not illuminated, thus avoiding the distortion they might cause to the beam.

Once reflected by the modulator the beam is resized by the telescope and enters the microscope. This telescope adapts the size of the beam to the objective pupil diameter. It comprises lenses L1 and L2 in Figure 1(a) and has a magnification of  $M_{tel} = -0.4$ . The focal lengths are, respectively,  $f_{L1} = 125$  mm and  $f_{L2} = 50$  mm. The beam fills up the objective pupil after being reflected by the dichroic mirror inside the microscope. The SLM is placed between polarizing elements, whose function is to polarize the incident and reflected light in such a way as to achieve the nearly phase-only configuration shown in Figure 3.

The microscope objective focal length can be obtained from its magnification ( $M=100X$ ). Figure 2 shows the objective and the visualization system. The lens that images the sample plane over the CCD camera is known as the tube lens. Its focal length is  $f'_{tube} = 200$  mm. The relationship between the objective focal length in air ( $f$ ),  $f'_{tube}$  and  $M$  is  $f = f'_{tube}/M = 2$  mm. The objective focal length in oil,  $f'$ , is obtained from the refraction index relationship:  $f' = fn = 2mm \cdot 1.51 = 3.02$  mm. The position of the exit focal length of the telescope and the objective pupil should be as coincident as possible to avoid light loss. The above mentioned factors are important in the hologram generation because they determine the scale factor between the modulator plane and the sample plane.

The dichroic mirror has a dual function: it reflects the laser beam into the objective and allows the sample visualization of the CCD camera by filtering the reflected laser, thus avoiding camera saturation. The CCD camera used in the experiment is a QICam Fast 1934 from QImaging.

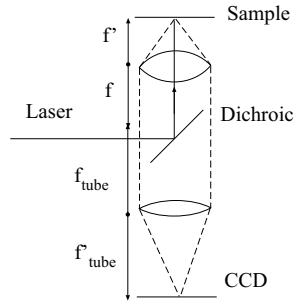


**Figure 2.** Objective-tube lens system in the microscope.

We have estimated the energy concentrated in one simple trap. The power concentrated in the sample plane is about a 25% of the incident power, taking into account the different transmittances of the optic elements and the efficiency of the modulation configuration.

### 2.1. Liquid Crystal Display HoloEye LCR2500

In this study we used a reflection twisted nematic LCoS (Liquid Crystal on Silicon). This offers phase modulation from 0 to  $2\pi$  in the configuration considered, although the phase is coupled with a certain amplitude variation. A summary of its technical specifications<sup>1</sup> is shown in the table 1. This modulator was chosen for its high resolution and minor cost when compared with other commercial devices.

Parameter	HoloEye LCR2500
In signal	XGA (1024×768 pixel)
Effective area	19.6×14.6 mm
Pixel size	19 $\mu\text{m}$ × 19 $\mu\text{m}$
Frame rate	72 Hz
Phase level modulation	$2\pi$ (400 nm-700 nm)

**Table 1.** Technical specifications of the HoloEye LCR 2500 modulator

The display was characterized with a beam incident direction of  $45^\circ$  from the normal device surface, as placed in the experimental setup (see Figure 1(a)). The best phase operating curve achieved is shown in Figure 3.

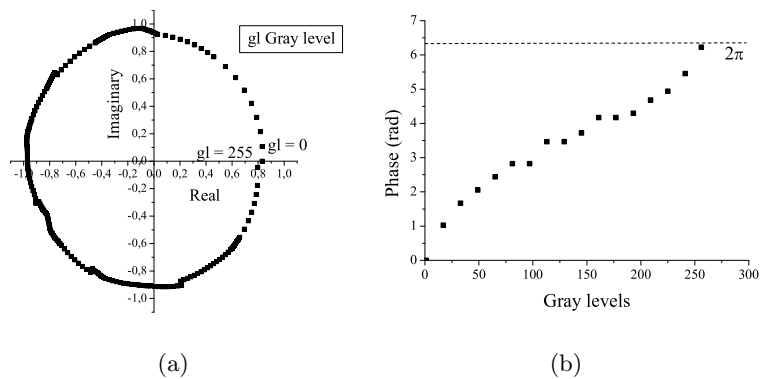


**Figure 3.** (a) HoloEye LCR 2500 phase operating curve obtained (b) Experimental phase values vs. gray level

This characterization was obtained with  $\lambda = 532$  nm, and the phase reaches  $2\pi$ . Its contrast is 1.25:1. The configuration efficiency is about 50%.

## 2.2. Aberration correction

The focalization of the beam in the microscope reveals two light lines instead of a diffraction limited spot. The two lines are perpendicular and appear at two different focal lengths. This behavior is similar to the presence of astigmatism, an aberration produced when a system converges at two different focal lengths. This kind of aberration is shown in Figure 4a.

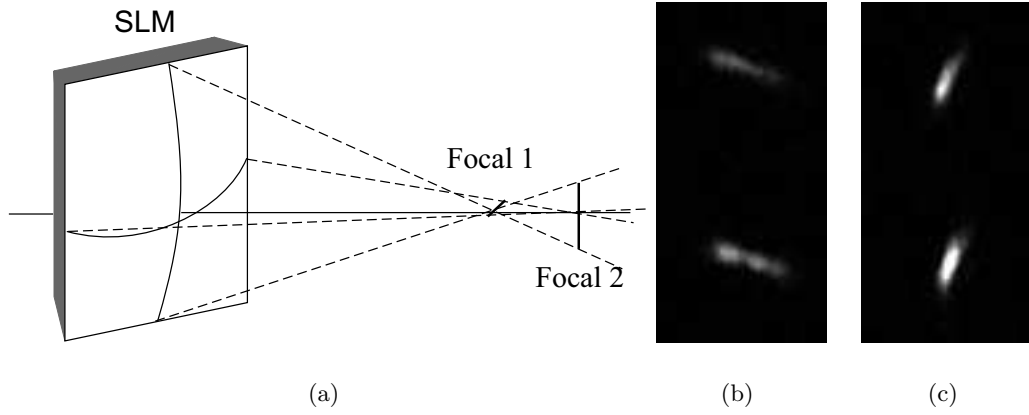


**Figure 4.** (a) Convergence of the reflected light from the modulator at two different focal lengths. (b) and (c) Experimental images showing two traps captured in the microscope in the Sturm focal lengths.

The light lines are known as Sturm focal lengths. Figures 4b and 4c show the captured images for the two Sturm focal lengths in the microscope for the generation of two traps. This behavior is shown even at normal incidence, thus revealing the lack of flatness of the device surface.

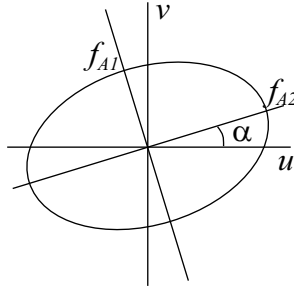


**Figure 5.** Correction of the modulator's aberration parameters

Let  $(u, v)$  and  $\alpha$  be the coordinates in the hologram plane and the angle between  $u$  and the direction in which the focal length  $f_{A1}$  is defined, respectively (see Figure 5). The aberration has been corrected by adding empirically a phase that counteracts it. The correction is dependent of focal lengths  $f_{A1}$ ,  $f_{A2}$  and  $\alpha$ . The phase function that corrects the aberration,  $\phi_{ab}$ , is modeled with the phase in equation 1.  $u'$  and  $v'$  are the  $\alpha$ -rotated axes of  $u$  and  $v$  (the modulator horizontal and vertical coordinates).

$$\phi_{ab} = -\frac{\pi}{\lambda} \left( \left( \frac{u'}{f_{A1}} \right)^2 + \left( \frac{v'}{f_{A2}} \right)^2 \right), \quad (1)$$

con  $u' = u \cos \alpha + v \sin \alpha$       and      y  $v' = v \cos \alpha - u \sin \alpha$ .

Experimentally, the parameters obtained were  $f_{A1} = 30$  m,  $f_{A2} = 8$  m and  $\alpha = 17^\circ$ . The resulting phase correction, adapted to the modulator operating curve (Figure 3 (b)), is shown in Figure 6(a). Figures 6(b) and 6(c) show the experimental captured images of the traps in the middle distance between the two Sturm focal lengths and the post-correction spots, respectively. An explanation of how to characterize and correct aberrations in an SLM can be found in reference.<sup>2</sup>

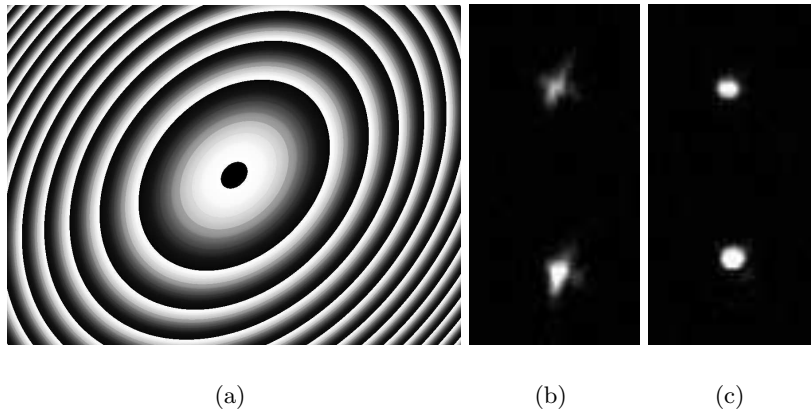


**Figure 6.** Spherical phase that corrects the HoloEye modulator aberration. Image of the two traps in the microscope (a) without correction (b) corrected.

### 3. DESCRIPTION OF THE INTERACTIVE APPLICATION

In this section we describe the hologram design process by means of a program that allows interactive manipulation with the sample. This software implements the random binary masks algorithm<sup>3</sup> for the fast generation of holograms and displays the distribution in the LCD in real time.<sup>4</sup>

The application is programmed in Java, a language that allows easy handling of the acceleration hardware capabilities and multi-threading programming. The program takes into account the experimental setup scale factors and different manipulation options, for example multiple vortex generation. The hologram generation includes the aberration correction and the experimental modulation of the LCD. A complete description of the application can be found in reference.<sup>5</sup>

The flowchart of the software is shown in Figure 7. It specifies the three block sources, the event handling class, the camera control class and the hologram calculation source. As an example, the flowchart shows the process of initializing the program, generating a trap and modifying its position.

The main thread of the program is responsible for the calculation and the interface event handling, whereas a second thread controls the camera and its related processes. The VolatileImage class, included in the Software Development Kit (SDK) of the Java Platform 5.0 is used to optimize the hologram displaying. This class takes advantage of the graphic hardware acceleration capabilities to display the images without using the CPU.<sup>6</sup> In this way, the calculation and the displaying of the holograms are parallel processes.

The integration of the camera, a QImaging QICam Fast 1394,<sup>7</sup> is achieved using the SDK provided by the manufacturer. Given that the SDK is designed to be used with C++, this library can be included in our

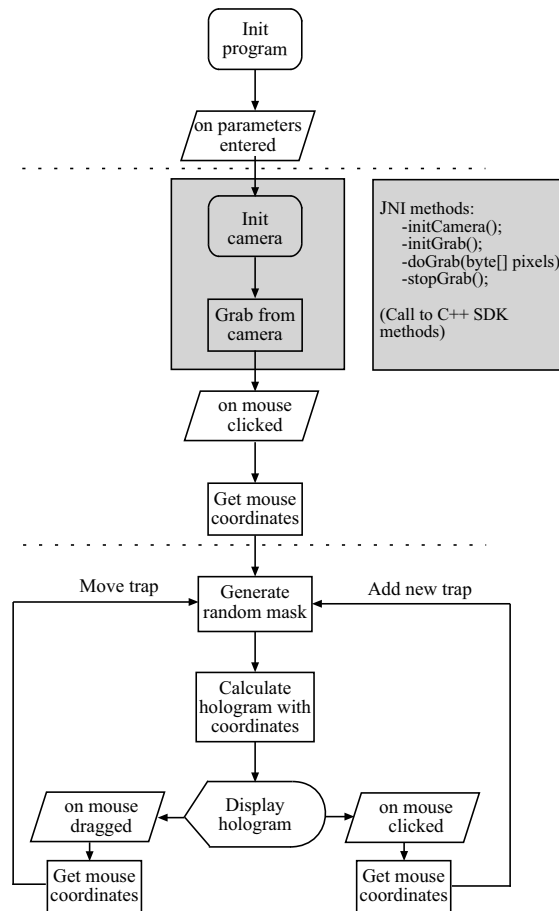


**Figure 7.** Flowchart of the interactive software.

Java software by using the Java Native Interface (JNI).<sup>8</sup> It allows calling to C or C++ functions from Java. A summary of the methods used to control the camera with the software is shown in Figure 7, while a more detailed description of JNI and the integration of FireWire cameras in Java can be found in reference.<sup>8,9</sup> A drawback of the program is that the FireWire camera that is not IEEE1394 compliant, and this limits the software that can be used with this specific camera.

Figure 8 shows the user interface of the application. The options included are:

1. the pixel size of the hologram,
2. the incorporation of the aberration correction and the modulator configuration through the *Init* button,
3. the selection of the trap to modify if there are several generated,
4. the possibility of modifying the trap depth with a slider,
5. multiple vortex generation,<sup>10</sup>
6. the button *Delete trap*, that is used to delete an undesired trap,
7. the user can change the hologram-generation method by clicking on the *RadioButton*. The two available methods are the *lenses and gratings*<sup>11</sup> and the *random binary masks*<sup>4</sup> methods.
8. the *Show/Hide grid* shows the scale in the microscope field.

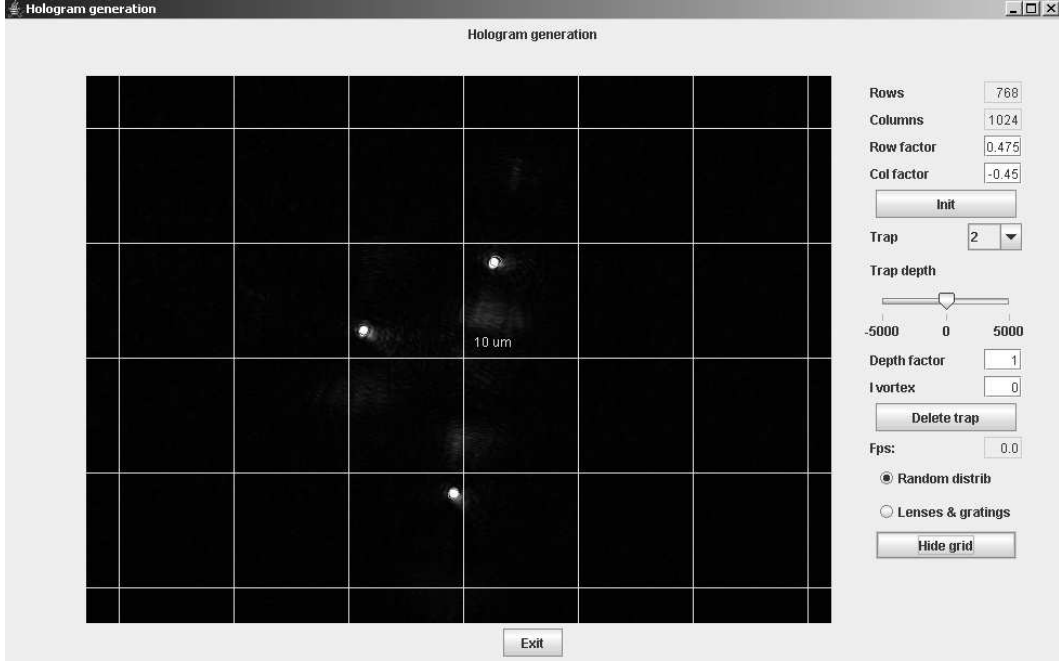


Figure 8. Main window program.

### 3.1. Hologram generation process

Once the user interface has been defined, it is necessary to study the steps involved in hologram generation. The modulator and the sample plane are related through a Fourier transform. In general, the hologram is complex-valued, and these values should be constrained to the experimental modulation available (see the operating curve shown in Figure 3). An off-axis trap is achieved with the function:

$$H(u, v) = \exp\left(i \frac{2\pi}{\lambda f} (ux_p + vy_p)\right), \quad (2)$$

where  $f$  is the effective focal length of the whole optical system. The Fourier transform of the linear phase in Equation 2 is  $\delta(x - x_p, y - y_p)$ . The sum of different phase grating functions will show multiple off-axis traps. To change the depth by a distance  $z$  from the focal plane a spherical phase has to be added to the desired linear phase function<sup>11</sup> (Equation 3).

$$H(u, v) = \exp\left(i \frac{\pi}{\lambda z} (u^2 + v^2)\right), \quad (3)$$

A hologram that combines multiple off-axis traps and/or displacements from the focal plane results in a non-phase distribution. There are different strategies to display a complex hologram using phase modulation such as the operating curve in Figure 3. We have used the random binary masks method, which divides the hologram into different pixel sets, each corresponding to a different trap. Each set will show the phase function that generates a single trap.<sup>3,4</sup>

The set of pixels that generates a trap is distributed at random in the hologram. Each set of pixels is called a random mask. The randomness is necessary to avoid the convolution of the trap with a geometric shape. Once the masks are generated, the phase corresponding to each trap is displayed in their disjoint masks. If a trap's coordinates are modified, only the phases in the trap mask have to be recalculated. This means that the calculation time does not increase if the trap number increases. Furthermore, no codification of the hologram distribution is needed because the function shown in each mask is a phase-only function. In contrast, the phases

and gratings method implies increased calculation time because the phase of the total distribution has to be computed.

The adjustment to the operating curve can be a time-consuming operation. To avoid this problem, we implemented a pre-calculated map that assigns a gray level to all the possible phases between 0 and  $2\pi$  by means of the minimum Euclidean distance of the phases. The resulting calculation time is equivalent to considering an ideal phase function. However, by not taking into account the experimental modulation there is a loss of quality in the trap pattern.

We have also evaluated the speed of program calculation. Taking into account the aberration correction and a hologram size of  $1024 \times 768$ , the full modulator resolution, the software achieves 12 fps\* when run on a Pentium IV HT, 3.2 GHz computer. If the resolution is  $512 \times 512$  and no aberration correction is needed, the program achieves up to 20 fps. The speed is enough to ensure interactive manipulation of the sample in both cases, and in addition to being independent of the operating curve characteristics it does not increase with the trap number.

### 3.2. Manipulation of yeast cells

In this section we report experimental results of particle manipulation in real time using the software developed. Figure 9 shows different captures of the manipulation of two yeast cells, approximately  $5 \mu\text{m}$  in diameter. First, a trap is generated to fix one cell position and thereafter another trap is used to move a second cell, moving it toward the first cell.

## 4. CONCLUDING REMARKS

We have presented a low-cost experimental setup designed to generate multiple dynamic holographic optical tweezers. The characteristics of the components have been explained in detail. The holograms displayed in the LCD are generated using a software that allows interactive manipulation, and which uses the random binary masks method. The performance of the software has been discussed and experimental results of trapped particles manipulated interactively have been reported.

## ACKNOWLEDGMENTS

This paper has been funded by the Spanish Ministry of Education and Science projects FIS2004-03450 and NAN2004-09348-C04-03.

## REFERENCES

1. [http://www.holoeye.com/download\\_datan/flyer\\_2500.pdf](http://www.holoeye.com/download_datan/flyer_2500.pdf), 2005.
2. K. D. Wulff, D. G. Cole, R. L. Clark, R. DiLeonardo, J. Leach, J. Cooper, G. Gibson, and M. J. Padgett, "Aberration correction in holographic optical tweezers," *Optics Express* **14**, pp. 4170–4175, 2006.
3. J. A. Davis and D. M. Cottrell, "Random mask encoding of multiplexed phase-only and binary phase-only filters," *Optics Letters* **19**, pp. 496–498, 1994.
4. M. Montes-Usategui, E. Pleguezuelos, J. Andilla, and E. Martín-Badosa, "Fast generation of holographic optical tweezers by random mask encoding of fourier components," *Optics Express* **14**, pp. 2101–2107, 2006.
5. E. Pleguezuelos, A. Carnicer, J. Andilla, and M. Montes, "Holotrap: a new software package for real-time optical trapping." Submitted to Computer Physics Communications. Available at <http://arxiv.org>, 2006.
6. <http://java.sun.com/j2se/1.5.0/docs/api/java/awt/image/VolatileImage.html>, 2004.
7. <http://www.qimaging.com/products/cameras/scientific/index.php>, 2004.
8. <http://java.sun.com/j2se/1.4.2/docs/guide/jni/index.html>, 2004.
9. B.-C. Lai, D. Woolley, and P. J. McKerrow, "Developing a java api for digital video control using the firewire sdk," *Proceedings AUC'2001*, pp. 9.1–8.9, (Townsville), 2001.
10. J. E. Curtis, B. A. Koss, and D. G. Grier, "Dynamic holographic optical tweezers," *Optics Communications* **207**, pp. 169–175, 2002.
11. J. Liesener, M. Reichert, T. Haist, and H. J. Tiziani, "Multi-funcional optical tweezers using computer-generated holograms," *Optics Communications* **185**, pp. 77–82, 2000.

---

\*frames per second



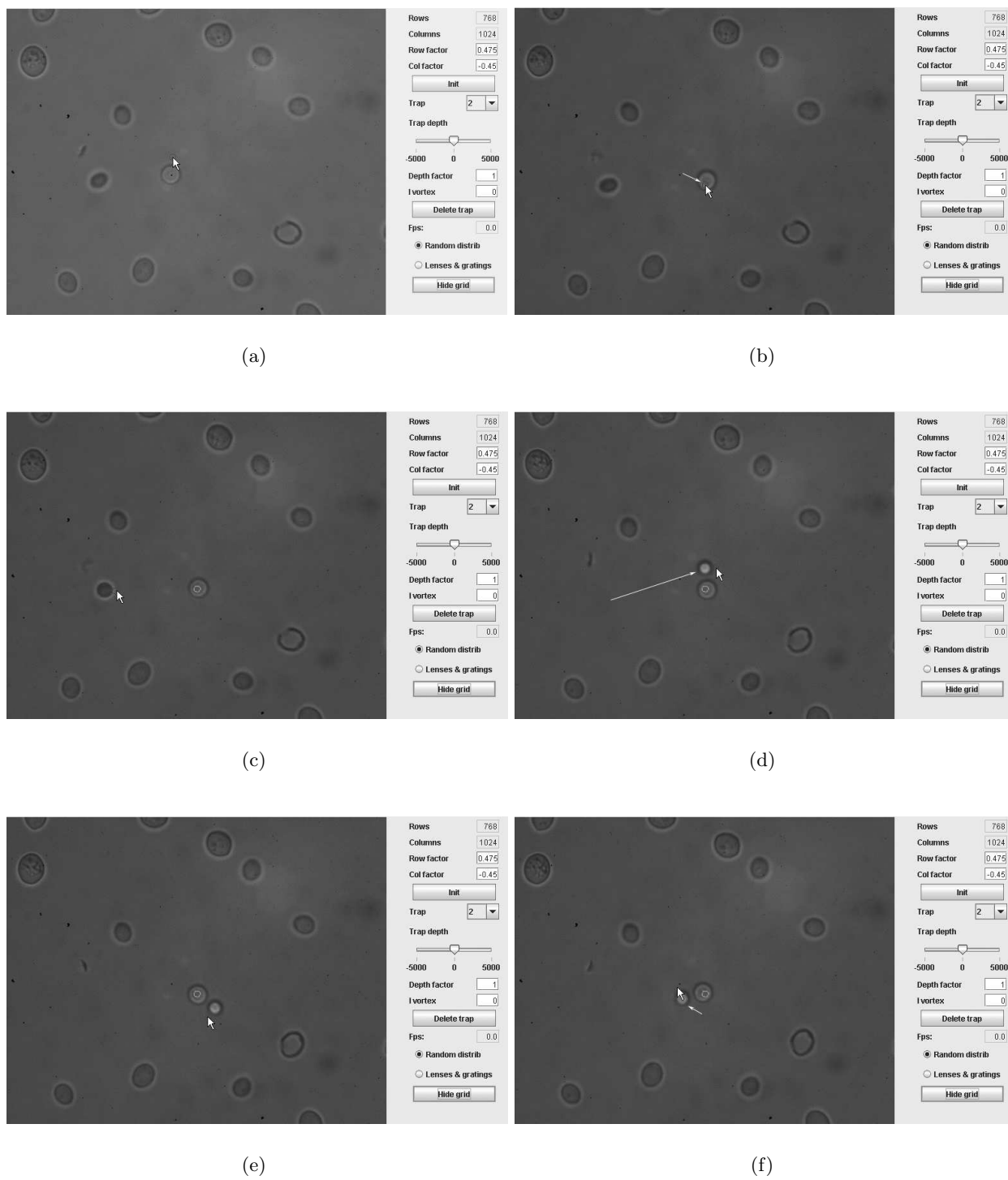


**Figure 9.** Experimental captures of the interactive manipulation of yeasts cells, using the software developed.